Dynamical response functions for the scalar phi ^{4}-lattice model near freezing temperature

1993 J. Phys.: Condens. Matter 5 5067

(http://iopscience.iop.org/0953-8984/5/29/005)

J. Phys.: Condens. Matter 5 (1993) 5067–5082. Printed in the UK

Dynamical response functions for the scalar φ^4-lattice model near freezing temperature

V L Aksenov†, E I Kornilov†‡ and J Schreiber‡§

† Frank Laboratory of Neutron Physics, JINR, 141980 Dubna, Russia
‡ Institute of Theoretical Physics, TU Dresden, O-8027 Dresden, Federal Republic of Germany

Received 4 January 1993, in final form 29 March 1993

Abstract. For the scalar φ^4-lattice model of structural phase transitions the freezing transition at a temperature T_c^* above T_c is found in the framework of mode-coupling theory. To study the critical behaviour of this transition the frequency and temperature dependencies of the linear and quadratic dynamical susceptibility are investigated by using a self-consistent numerical solution of the mode-coupling equations. Two cases are considered: (i) a pure crystalline system with a B transition at T_c^*, and (ii) a system with randomly distributed defects with an A transition at T_c^*. The experimental aspects of the presented results are discussed.

1. Introduction

In crystalline systems with a structural phase transition some anomalous behaviour can be observed above the transition temperature T_c [1,2]. In perovskites, for example, the classical soft-mode picture of structural phase transitions breaks down and precursor fluctuations give rise to an extra very narrow central peak in the order parameter fluctuation spectrum [2,3]. In addition to many attempts to explain the appearance of correlated clusters (precursors) a concept has been developed [4,5] that is similar to that for the dynamical glass transition suggested by Götze and co-workers [6] on the basis of mode-coupling theory. According to this theory in pure crystalline systems an ideal narrow (static) central peak must set in at the so-called freezing temperature T_c^*. This transition is accompanied by an appearance of finite long-time correlations of the local atomic displacement $u_i = Q_i - \langle Q_i \rangle$, i.e.

$$L_{i,j} = \lim_{t \to t_\infty} \langle u_i(t) u_j(0) \rangle \neq 0 \qquad T \leqslant T_c^* \tag{1}$$

where $\langle \cdots \rangle$ denotes the thermodynamic average. In mode-coupling theory the limit in (1) means strictly $t_\infty \to \infty$. This would imply an ergodicity breaking [4,7]. For improved approaches dealing with realistic systems, (1) should be formulated with a large experimentally and theoretically accessible timescale t_∞. Characteristic values of t_∞ may range from 10^{-8} s to a few seconds, according to the kind of system being investigated. The disadvantage of such a condition is that the transition temperature T_c^* is not well defined. Therefore (1) is not suitable to prove the mode-coupling results experimentally. It is the task

§ Present address: Fraunhofer Institute for Nondestructive Testing, University of the Saarland, Building 37, D-66123 Saarbrücken 11, Federal Republic of Germany.

0953-8984/93/295067+16$07.50

of this paper to draw attention to experimentally significant characteristics of a transition at T_c^*†.

Thus, in a formal sense, the physical situation at $T > T_c$ in the systems with a structural phase transition reminds one of supercooled liquids or polymers above the glass transition point T_g [9, 10]. In recent years, with mode-coupling theory at hand, substantial progress has been made in the understanding of the freezing process near the glassy transition. The main result was the prediction of the dynamical glass transition temperature $T_c^* \simeq T_g + \Delta T$, where ΔT is about 50 K. At this temperature the intensity of the quasistatic central peak in the density fluctuation spectrum and the dynamical density response function exhibits critical scaling behaviour in certain frequency regions [6, 10, 11]. This prediction was partly verified in a number of experiments with glassy materials [10, 12–16].

Following this idea, it would be interesting to look at $T_c^* > T_c$ for some experimental confirmation of the existence of the freezing transition in crystalline systems. Simultaneously, the question may arise as to whether, in systems with transitions into structural, dipole, orientational, spin, quadrupole or any other glassy states, the dynamic freezing transition can be observed above the thermodynamic glass transition temperature T_g[17, 18]. To answer this question, investigation of the intensity of the central peak is not sufficient, as some kind of hopping processes could smear the central peak near $T \leqslant T_c^*$, making impossible unambiguous identification. The presence of static or relaxing defects would mask the central peak of intrinsic dynamical origin [17]. Therefore, the analysis of the dynamical response functions at not too low frequencies is more suitable as a test of the critical scaling behaviour at T_c^*. This has successfully been done for glasses [16].

This paper presents a numerical calculation, made in the framework of mode-coupling theory, of the frequency and temperature dependence of the real and imaginary part of the dynamical susceptibility near the freezing transition. The calculation was performed for the scalar φ^4-lattice model of structural phase transitions. The mode-coupling equations for the isothermal relaxation function were solved directly in real-time space. The resulting integro-differential equation was handled by the predictor–corrector method, and the time evaluation over five time decades was analysed.

We hope that the theoretical results presented will stimulate a detailed experimental search for the freezing transition at temperatures above T_c (or T_g) in crystalline systems. This could be done by neutron and light scattering methods or dielectric and magnetic relaxation measurements.

2. Model and mode-coupling equations

The scalar φ^4-lattice model is determined by the Hamiltonian [3, 19]

$$H = \sum_i (\tfrac{1}{2} P_i^2 - \tfrac{1}{2} A_i Q_i^2 + \tfrac{1}{4} B_i Q_i^4) + \frac{1}{4} \sum_{ij} C_{ij} (Q_i - Q_j)^2 \tag{2}$$

where Q_i is the coordinate of the local normal mode that determines the structural phase transition. Within the elementary cell Q_i can be considered as the coordinate of the effective particle of mass $m = 1$, moving in a double-well potential; P_i is then the conjugate

† We note that the mode-coupling scenario is not the only one describing freezing transitions. It is known that ergodicity breaking may have structural or dynamical reasons [7]. Therefore we believe that in certain systems, e.g. in orthoterphenyl [8], freezing anomalies will be observed at the thermodynamic glass transition (at $T_g < T_c^*$) as well as at the dynamical freezing transition (at T_c^*).

momentum of this particle. The interaction between the particles occupying different lattice cells of a three-dimensional lattice ($i = 1, \ldots, N$) is then described by the harmonic force constants C_{ij}. In the pure crystalline case the parameters of the Hamiltonian are independent of the cell number, but in quenched disordered systems they can be random. To study the influence of defects on the phase transition, only the parameters A_i are assumed to be site random ($B_i = B$). Following [5] let us consider $A_i = A_D \gtrless 0$ at defect sites and $A_i = A > 0$, otherwise. If p is the defect concentration, then the probability distribution of A_i looks like

$$P(A_i) = p\,\delta(A_i - A_D) + (1 - p)\delta(A_i - A). \tag{3}$$

To study the relaxation processes in the model we introduce the averaged isothermal relaxation function

$$\Phi_{lk}(t) = (u_l(t)|u_k) = \int_0^\beta \mathrm{d}\beta' \overline{\langle u_l(t - \mathrm{i}\beta')u_k\rangle} \qquad \beta = 1/k_B T \tag{4}$$

where $u_l(t) = Q_l(t) - \langle Q_l\rangle$ is the displacement operator, the bar denotes the configurational average over the random quantities A_i, and $\langle\cdots\rangle$ is the thermodynamical average taken over canonical ensemble. Hereinafter we use units with $\hbar = 1$. The initial value of $\Phi_{lk}(t)$ determines the static isothermal susceptibility $\chi_{lk}^T = \Phi_{lk}(t = 0)$. By introducing the Laplace transform of $\Phi_{lk}(t)$ in the form

$$\Phi_{lk}(z) = \mathrm{i}\int_0^\infty \mathrm{d}t\mathrm{e}^{\mathrm{i}zt}\Phi_{lk}(t) \equiv ((u_l|u_k)) \qquad \mathrm{Im}z > 0 \tag{5}$$

the following exact q-representation can be derived by the equation of motion and using the Mori-projection formalism [20]:

$$\Phi_q(z) = -\chi_q^T\left(z - \frac{1/\chi_q^T}{z + M_q(z)}\right)^{-1} \tag{6}$$

where $\Phi_{lk}(z) = (1/N)\sum_q \Phi_q(z)\exp[\mathrm{i}q(R_l - R_k)]$. The relaxation kernel $M_{lk}(z)$ is given by

$$M_{lk}(z) = ((\ddot{Q}_l|\ddot{Q}_k))_{(2)} \tag{7}$$

where the lower index $_{(2)}$ denotes the projection procedure to be done in the way suggested by Tserkovnikov [4, 21]. In the spirit of the mode-coupling approximation the relaxation kernel is estimated with the expression that comes from factorization of u_i powers and truncation of the configurational average in (7), as in [5]. For the classical limit ($\Phi_{lk}(t) \Longrightarrow \beta\langle u_l(t)u_k(0)\rangle$) we get

$$M_{lk}(t) = v_1\Phi_{lk}(t) + v_3\Phi_{lk}{}^3(t). \tag{8}$$

The coupling parameters are determined in the following way:

$$v_1 = A^2 p(1 - p)(1 - A_D/A)^2 \qquad v_3 = 6B^2 k_B^2 T^2. \tag{9}$$

To get large values for v_1, even for small concentrations p, strong harmonic defects ($|A_D| \gg A$) are necessary.

To simplify further calculations we exploit the fact that the critical scaling law does not essentially depend on relaxation function dispersion [10, 22]. Therefore, to qualitatively investigate the freezing dynamics picture at T_c^* we neglect the relaxation kernel dispersion, i.e. $M_{lk}(t) \approx \delta_{lk} M(t)$. Then, self-consistent determination of a diagonal or local part of the relaxation function becomes possible, if we use the following ansatz for the isothermal susceptibility:

$$\chi^T = \chi_{ll}^T = \frac{1}{N} \sum_q \chi_q^T = \frac{1}{\omega_0^2} \tag{10}$$

where ω_0^2 has the form

$$\omega_0^2 = A\tau + C \qquad \tau = (T - T_c)/T_c \tag{11}$$

and $C = \sum_j C_{ij}$. The ansatz (10) is in accord with Landau theory and will be a reasonable approximation inside the non-critical region with respect to the structural phase transition. Within this approach the critical temperature can be estimated as $T_c = \frac{1}{3} f_0 T_0$ [5], where $f_0 = C/A$ is the dimensionless coupling parameter and $T_0 = A^2/Bk_B$ is some unit of temperature expressed through model parameters. We then assume that τ_c^* lies outside the critical fluctuation region, as the mode-coupling theory for the freezing transition (also for the dynamical glass transition) assumes no critical fluctuations at T_c [4, 10].

It is worth emphasizing that, in spite of (10), we do not consider the case of an infinite interaction radius, i.e. $C_{ij} = C/N$. Then the model is solvable and, as is shown in [23], at $C/A < 1$ the quantity $L_{ii}(T)$ tends to zero only if $T \to \infty$, and only at $C/A > 1$ vanishes. Of course, the freezing transition is expected only for systems with a finite interaction radius [24–26]. The approximation used above should be considered as an approximation valid for systems where the freezing transition really exists. Within our theory we cannot prove the existence of such a transition. However, if this transition exists, the presented mode-coupling theory may give a good guideline for the experimentalists in the same way that mean-field theory does in the case of usual phase transitions.

Thus it is possible to rewrite (6) in the time representation. On carrying out Laplace back-transformation of (6) and taking into account (8)–(11) one can obtain the following equation:

$$\ddot{\Phi}(t) + \omega_0^2 \Phi(t) + \int_0^t \mathrm{d}\tilde{t} \dot{\Phi}(t - \tilde{t}) M(\tilde{t}) = 0 \tag{12}$$

with the initial conditions

$$\Phi(0) = \chi^T \qquad \dot{\Phi}(0) = 0. \tag{13}$$

It is convenient to express (12) through dimensionless variables and parameters. Introducing the new function $D(t) = \Phi(t)/\chi^T$, it takes the form

$$\ddot{D}(t) + \omega_0^2 D(t) + \int_0^t \mathrm{d}\tilde{t} \dot{D}(t - \tilde{t}) M(\tilde{t}) = 0 \tag{14}$$

with the initial conditions

$$D(0) = 1 \qquad \dot{D}(0) = 0. \tag{15}$$

For the sake of convenience in what follows we will also use the dimensionless frequency and time variables, i.e. $\omega \to \omega/A^{1/2}$ and $t \to tA^{1/2}$. Within this notation we have $\omega_0^2 = \tau + f_0$.

If no direct measurement of linear susceptibility is possible, then the observed quantities, like damping and the velocity of ultrasonic waves, have contributions from several non-linear response functions. To follow the influence of these contributions let us consider the quadratic susceptibility

$$\chi_{(2)}(\omega) = \omega \mathrm{LT}[(u_i^2(t)|u_i^2(0))] \tag{16}$$

where $\mathrm{LT}[F(t)]$ means the Laplace transform of $F(t)$. To estimate (16) the factorization procedure used for the approximation of the relaxation kernel can be employed. Neglecting a contribution of the correlation functions of the type of $((u_i^2|u_i))$ and $((u_i^2|\dot{u}_i))$ to $((u_i^2|u_i^2))$, the latter can be approximated by $((u_i^2|u_i^2))_{(2)}$, and then the quadratic susceptibility can be presented in the following way:

$$\chi_{(2)}(\omega) = -\frac{1}{2\pi}\int \mathrm{d}\tilde{\omega}\frac{\mathrm{e}^{\beta\tilde{\omega}}-1}{\omega-\tilde{\omega}}\int \mathrm{d}t\mathrm{e}^{-\mathrm{i}\tilde{\omega}t}2\langle u(t)u\rangle^2. \tag{17}$$

To solve the above equations one needs to apply an appropriate numerical procedure. In the next section we describe a suggested method for the solution of the integro-differential equations like (14).

3. The numerical procedure

Let us consider the general form of the memory integro-differential equation of second order. With the abbreviation $m(t) \equiv M(t)/\omega_0^2$ and adding a small phenomenological microscopic relaxation term one obtains the relaxation equation in the following form:

$$\ddot{D}(t) + \nu\dot{D}(t) + \omega_0^2 D(t) + \omega_0^2\int_0^t \mathrm{d}\tilde{t}\dot{D}(t-\tilde{t})m(\tilde{t}) = 0 \tag{18}$$

with the initial conditions

$$D(0) = 1 \qquad \dot{D}(0) = 0. \tag{19}$$

The memory-type equations like (12) and (18) appear in numerous theoretical studies of dynamic phenomena. For instance, the theory of long-time relaxation processes in supercooled liquids [10] is based mostly on the analysis of the behaviour of the solutions of these integro-differential equations. The specific behaviour of the dynamic response functions can be described by solving (18) with an appropriately chosen kernel $m(t)$ as the polynomial in $D(t)$:

$$m(t) = \mathcal{F}\{D(t)\} = \sum_n \tilde{v}_n D^n(t). \tag{20}$$

Comparing with (8) the parameters $\tilde{v}_n$ are given for the scalar φ^4-lattice model by the following equations:

$$\tilde{v}_1 = v_1/\omega_0^4 = (\tau + f_0)^2 p(1-p)(1 - A_D/A)^2$$
$$\tilde{v}_3 = v_3/\omega_0^8 = (\tau + f_0)^4 (T/T_0)^2 \qquad \tilde{v}_2 = \tilde{v}_{n\geqslant 4} = 0.$$

The widely used method [10] for solving (18) can be briefly described as follows.

(i) The trial function $D^{[0]}(t)$ is taken inside some appropriate time domain.
(ii) The relaxation kernel $m^{[k]}(t) = \mathcal{F}\{D^{[k]}(t)\}$ is calculated (with $k = 0$ in the first step).
(iii) The Laplace transforms of both the correlator $D^{[k]}(z) = \mathrm{LT}\{D^{[k]}(t)\}$ and the relaxation kernel $m^{[k]}(z) = \mathrm{LT}\{m^{[k]}(t)\}$ are performed.
(iv) The next approximation for the correlator $D^{[k+1]}(z)$ is obtained according to (6):

$$D^{[k+1]}(z) = -\left(z - \frac{\omega_0^2}{z + \mathrm{i}\nu + \omega_0^2 m^{[k]}(z)}\right)^{-1}. \tag{21}$$

(v) The back Laplace transform (BLT) is used for obtaining the approximate solution $D^{[k+1]}(t) = \mathrm{BLT}\{D^{[k+1]}(z)\}$.
(vi) The integral convergence criterion is used to decide on whether to stop the iteration procedure or to continue the calculation from (ii).

Although Laplace transforms of almost any function are now relatively simple to do numerically on a small supercomputer [27], problems remain in solving the above-described self-consistent procedure. In this connection the authors in [28] found that "this procedure is not practical...since Laplace transforms are very cumbersome for functions, which are structured and stretched on such large windows...". In the present paper we suggest a different numerical approach to the solution of (18). This method in the theory of ordinary differential equations is called the predictor–corrector method [29, 30]. The method consists in doing the following subsequent steps.

First, we obtain the Taylor expansion of the unknown function near $t = 0$ up to seventh order in t

$$D(t) = 1 + a_2 t^2 + a_3 t^3 + \ldots + a_7 t^7 \tag{22}$$

in order to explore this precise series in finding a solution at the first few steps of the integration scheme. The coefficients a_k are determined after substituting (22) into (18). The initial conditions were already used in (22).

Application of the predictor–corrector method to the second-order integro-differential equation means a splitting of the original equation into a system of two first-order equations by introducing the new function $P(t) = \dot{D}(t)$. Then we can write the system in the following 'standard' form:

$$\dot{P}(t) = F\{D(t), P(t)\} \qquad \dot{D}(t) = G\{D(t), P(t)\} \tag{23}$$

with the initial conditions $P(0) = 0$, $D(0) = 1$. Here we introduce

$$F\{D(t), P(t)\} = -\nu P(t) - \omega_0^2(D(t) + I(t)) \qquad G\{D(t), P(t)\} = P(t)$$

where the integral part is

$$I(t) = \int_0^t \mathrm{d}\tilde{t}\, P(\tilde{t}) m(t - \tilde{t}) \tag{24}$$

with $m(t)$ defined by (20). Then we introduce the grid representation of all functions in the form $D_i = D(t_i)$, $P_i = P(t_i)$, $m_i = m(t_i)$, with a discrete time $t_i = ih$ expressed through stepsize h. To predict the values of D_{i+1} and P_{i+1} we use

$$P_{i+1}^{(0)} = P_{i-1} + 2hF\{D_i, P_i\} \tag{25}$$

$$D_{i+1}^{(0)} = D_{i-1} + 2hG\{D_i, P_i\} \tag{26}$$

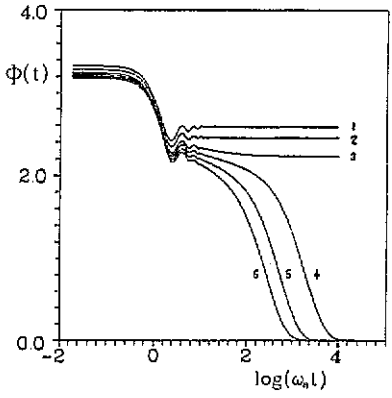

Figure 1. The time dependence of the relaxation function $\Phi(t)$ of the F_3 model for different temperatures τ. τ = 0(1); 0.004(2); 0.008(3); 0.010(4); 0.012(5); 0.014(6). The freezing temperature $\tau_c^* \approx 0.0083$ for this set of model parameters.

and make corrections according to iteration over k

$$P_{i+1}^{(k+1)} = P_i + \tfrac{1}{2}h(F\{D_i, P_i\} + F\{D_{i+1}^{(k)}, P_{i+1}^{(k)}\}) \tag{27}$$

$$D_{i+1}^{(k+1)} = D_i + \tfrac{1}{2}h(G\{D_i, P_i\} + G\{D_{i+1}^{(k)}, P_{i+1}^{(k)}\}) \tag{28}$$

while the convergence criterion $[(D_{i+1}^{(k+1)} - D_{i+1}^{(k)})^2 + (P_{i+1}^{(k+1)} - P_{i+1}^{(k)})^2]^{1/2} \leqslant \varepsilon$ is satisfied. One of the advantages of the predictor–corrector method consists in the fact that a more exact calculation of the correlation function $D(t)$ near the beginning of the t axis is due to the use of this very point convergence criterion. We then take into account a simple estimate of the discretization error of the predictor–corrector method [30] by

$$\delta P_{i+1} = \tfrac{1}{5}(P_{i+1}^{(0)} - P_{i+1}^{(k+1)}) \qquad \delta D_{i+1} = \tfrac{1}{5}(D_{i+1}^{(0)} - D_{i+1}^{(k+1)}) \tag{29}$$

and use (29) to obtain the final correction for the solution (27), (28).

It is necessary to say a few words about the calculation of the integral part $I(t)$. In choosing a scheme of numerical integration it is necessary to take into account the complex estimate of calculational difficulty. On one hand, there exist many numerical methods of enhanced precision (h^3 or higher order) but all of them require larger-volume calculations with increasing accuracy. On the other hand, to find solutions at every new time point t_i, it is necessary to recalculate (24). Since usually we need about 10^3–10^4 points in a time domain, it appears suitable to use the simplest scheme of the first order in h:

$$I_i = \tfrac{1}{2}h(P_0 m_i + P_i m_0) + h\sum_{j=1}^{i-1} P_j m_{i-j}. \tag{30}$$

This notation illustrates another advantage of this scheme, namely that in the stage of making the correction iteration the sum is calculated only once.

Finally, once the dimensionless solution $D(t)$ is obtained within a suitable time domain, we renormalize it to operate in the following with the mode coupling correlator $\Phi(t)$. This transformation is the reverse transformation to that we used for deriving (14) from (12). Further numerics are standard rather than new. Thus, for example, we performed Laplace transform of the correlators by the Filon algorithm [31]. The numerical method proposed can easily be realized on any type of modern computer. We made use of a VAX-8650, where typical CPU times were about 10–20 minutes per run. At the vicinity of the freezing transition the calculation of each curve took around two hours.

4. Results and discussion

The time-dependent local relaxation function $\Phi(t)$ from (12) is shown in figure 1 for the case $v_1 = 0 (p = 0)$ (the F_3 model in Götze's notation [10]), $f_0 = 0.3$ and $T_c = 0.1T_0$. The time evolution can be followed over nearly six decades. Since $\tau < \tau_c^* \approx 0.0083$, the function $\Phi(t)$ has a finite value for $t \to \infty$ in agreement with the result directly obtained from (6), if one takes the limit $L_{ii} = \lim_{z \to i0} z\Phi_{ii}(z)$ [5]. The value $l_c^* = L_{ii}(\tau_c^*)/\chi^T(\tau_c^*) = \frac{2}{3}$ (a discrete B transition [10]). For $\tau > \tau_c^*$ two characteristic relaxation regions can be distinguished: when $\Phi(t) \sim 2.0$ it is the β relaxation, and the region when $\Phi(t) \to 0$ belongs to α relaxation. To obtain more information about both relaxation regions the Laplace transform of $\Phi(t)$ should be studied. In figures 2 and 3 the real and imaginary part of the dynamic susceptibility

$$\chi(\omega) = \omega \, \mathrm{LT}[\Phi(t)](\omega) \tag{31}$$

for the F_3 model are shown. It can be seen that the linear and quadratic susceptibility have nearly same qualitative ω and T dependencies. From these curves a qualitative representation of the scaling laws of α relaxation ($\omega \sim 10^{-3}$) and β relaxation ($\omega \sim 10^{-1}$) can be derived. Götze [10, 32] found the analytical expressions for these scaling laws from (6) and (8) using $\epsilon = (T - T_c^*)/T_c^*$, as the small expansion parameter, and considering the $\omega \to 0$ limit. For $\epsilon > 0$ two frequency scales $\omega_\alpha \sim \epsilon^{1/2a+1/2b}$ and $\omega_\beta \sim \epsilon^{1/2a}$ separate the α and β relaxation. Around ω_β the simple interpolation formula

$$\chi''(\omega) \approx \sqrt{\epsilon}\,[\Gamma(1-a)\,\sin(\pi a/2)\,(\omega/\omega_\beta)^a + B\,\Gamma(1+b)\,\sin(\pi b/2)\,(\omega_\beta/\omega)^b] \tag{32}$$

can give a good approximation to the susceptibility behaviour illustrated in figure 3. Unlike the usual phase transition case the exponent parameters a and b are not the universal ones and depend on model parameters and, hence, on temperature. According to [32] these parameters are determined by the equation

$$\Gamma^2(1-a)/\Gamma(1-2a) = \Gamma^2(1+b)/\Gamma(1+2b) = \lambda(T) \tag{33}$$

where $\Gamma(x)$ is the Gamma function. The exponent parameter $\lambda(T)$ is given by

$$\lambda(T) = 3\,(1 - l_c)^3\, v_3\, l_c \qquad l_c = \beta L_{ii}(T)/\chi^T(T). \tag{34}$$

In figure 4 the quantities $l_c(T)$, $\lambda(T)$, $a(T)$ and $b(T)$ are shown as the functions of temperature.

Another insight into scaling behaviour can be gained by considering the temperature dependence of $\chi''(\omega, T)$ at fixed frequency ω. This is the typical experimental situation, for example, with Brillouin scattering. The corresponding results are plotted in figure 5. Unfortunately, these curves show that the T dependence of $\chi(\omega, T)$ lacks sensitivity for the experimentalists to detect anomalous critical behaviour at T_c^*. For example, for $\epsilon < 0$, $\chi''(\omega, T) \sim \omega|\epsilon|^{-1/2a+1/2}$ was predicted by the theory. One has to remember, also, that T_c^* is very close to T_c in the pure B-type transition case [4, 5] and no definite conclusion about the freezing transition in pure systems can be drawn from such experiments.

Let us now consider the F_{13} model ($v_1 \neq 0$) arising when one includes the non-zero defect concentration $p \neq 0$. To enlarge the interval between T_c and T_c^* we take $v_1 = 6.25A^2$ and $f_0 = 2.1$, corresponding to $T_c = 0.7\,T_0$ and $T_c^* = 0.98\,T_0$ or $\tau_c^* = 0.4$. As we choose the control parameter v_1 large enough the freezing transition changes its type, i.e. now

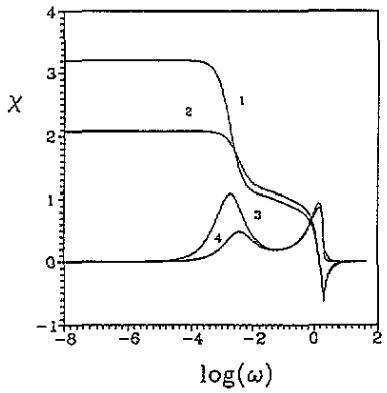

Figure 2. The frequency dependence of the real (1: χ' and 2: $\chi'_{(2)}$) and imaginary (3: χ'' and 4: $\chi''_{(2)}$) part of the susceptibility of the F_3 model for the temperature $\tau = 0.012 > \tau_c^*$. The odd and even labels correspond to a linear and quadratic part of the susceptibility, respectively. See text for details.

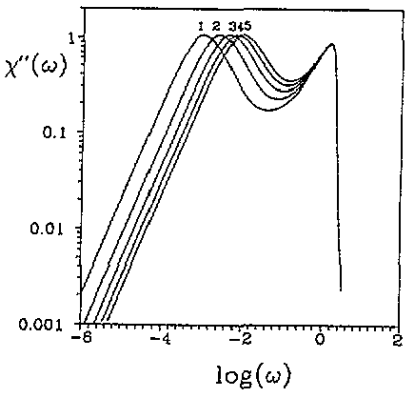

Figure 3. The imaginary part of susceptibility $\chi''(\omega)$ of the F_3 model against $\log(\omega)$ for different temperatures τ.

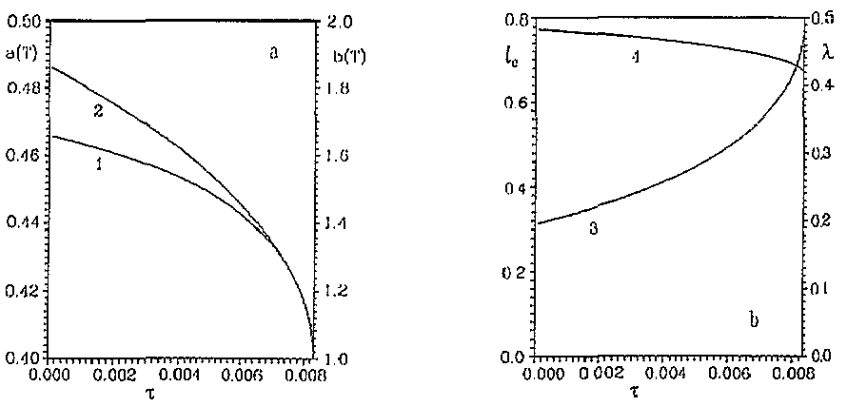

Figure 4. (*a*) The characteristic exponents a (1) and b (2), and (*b*) the exponent parameter λ (3), and the non-ergodic constant l_c (4), against temperature for the F_3 model.

$L_{ii}(\tau \to \tau_C^*) \to \epsilon \to 0$ (the A transition [10]). Due to this continuous transition no freezing of the α peak occurs, as shown in figure 6. There is no α peak at all. The scaling behaviour is now restricted to β-like relaxation at $\omega \sim \omega_\beta \sim \epsilon^{1/a'}$: $\chi''(\omega) \sim \omega\epsilon^{1-1/a'}$ for $\omega \ll \omega_\beta$ and $\chi''(\omega) \sim \omega^{a'}$ for $\omega \gg \omega_\beta$. The temperature dependence of the parameter a' is shown in figure 7 (see (33)). From the double logarithmic plot of $\chi''(\omega)$ in figure 6 it follows that the analytical scaling laws are not quite illustrative in such a presentation. On the other hand, the critical temperature behaviour of $\chi''(\omega, \tau)$ at fixed frequency is clearly seen in a relatively wide frequency window (see figure 8). For rather different frequencies $\chi''(\omega, \tau)$ has a pronounced peak at τ_c^*. The peak becomes the broader the higher the frequency. Nevertheless, for $T < T_p^-$ and $T > T_p^+$, where T_p is determined by $\omega = \omega_\beta(T_p)$, the scaling

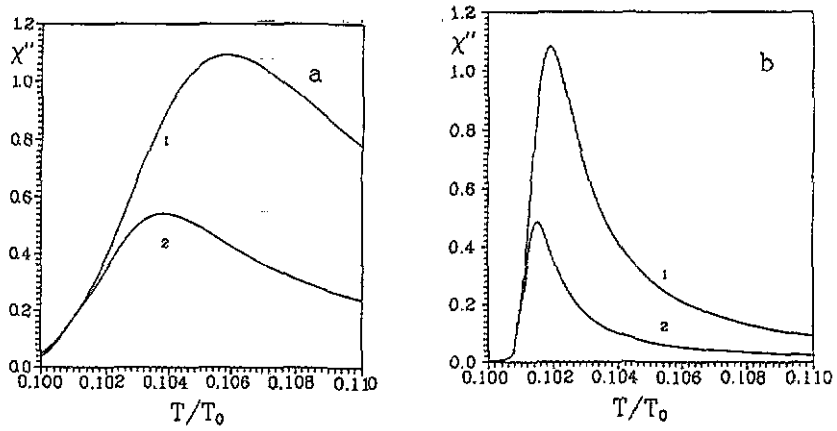

Figure 5. *The imaginary part of the linear* χ'' (1) *and quadratic* $\chi''_{(2)}$ (2) *susceptibility against temperature for the* F_3 *model for* $\omega = 0.1$ (*a*) *and* $\omega = 0.01$ (*b*). *The model parameters are* $T_c = 0.1T_0$ *and* $\tau_c^* \approx 0.0083$.

law $\chi''(\omega, T)/\omega \sim \epsilon^{1-1/a'}$ can be sufficiently well recognized, if the measuring frequency is not too high (see figure 9). Here the influence of the quadratic susceptibility $\chi_{(2)}(\omega)$ is not drastic and in the region of the scaling law validity ($T < T_p^-$ and $T > T_p^+$) $\chi''_{(2)}(\omega, T)$ is a nearly flat function of temperature. Therefore, the critical behaviour in $\chi''(\omega, T)$ is not masked with quadratic susceptibility, if the measured quantity is influenced by both susceptibilities.

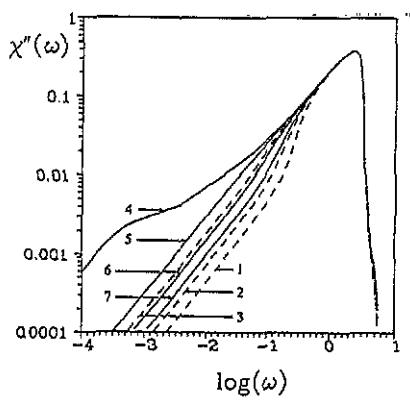

Figure 6. The imaginary part of the susceptibility $\chi''(\omega)$ of the F_{13} model against $\log(\omega)$ for different temperatures τ. τ = 0(1); 0.10(2); 0.25(3); 0.40(4); 0.50(5); 0.60(6); 0.70(7). Broken curves correspond to a non-ergodic regime, whereas full curves correspond to the temperatures $\tau \geqslant \tau_c^* = 0.40$.

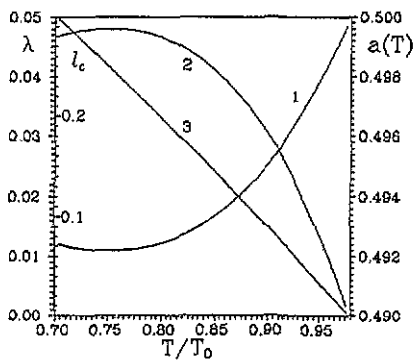

Figure 7. The characteristic exponent a' (1), the exponent parameter λ (2), and the non-ergodic constant l_c (3) against temperature for the F_{13} model.

At the same time as $\chi''(\omega, T)$ shows a peak at τ_c^* the real part $\chi'(\omega, T)$ changes its slope at τ_c^* and a cusp-like behaviour is observed, more clearly at lower frequencies, up to $\omega \to 0$ (see figure 8). This feature of the A-type freezing transition reminds us of the spin-glass

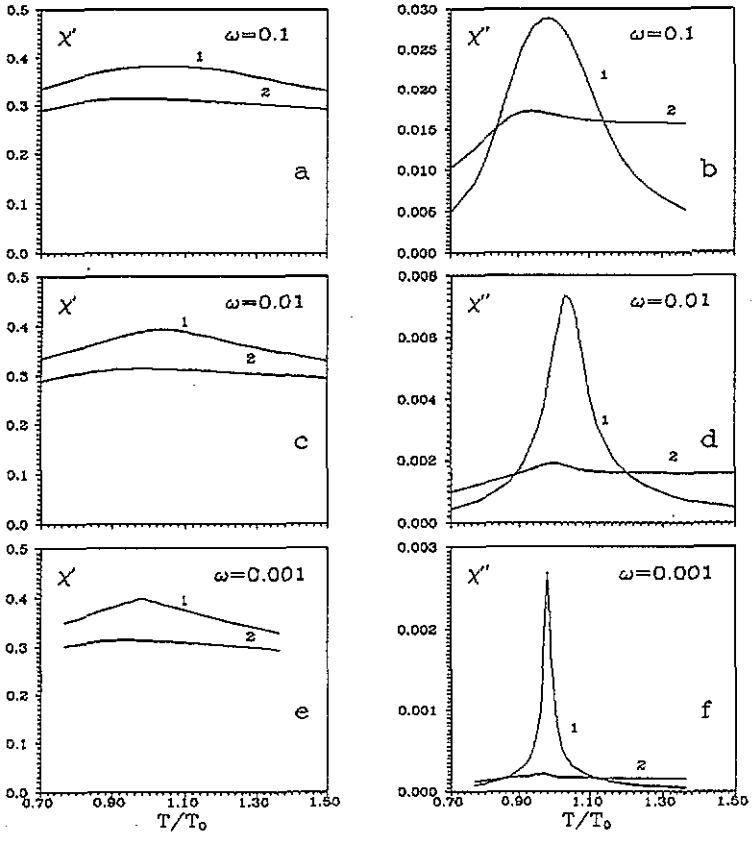

Figure 8. The temperature dependence of the real χ' (a, c, e) and imaginary χ'' (b, d, f) parts of the susceptibility of the F_{13} model for the frequencies $\omega = 0.1$, 0.01, 0.001. The labels 1 and 2 correspond to the linear and quadratic parts of susceptibility, respectively.

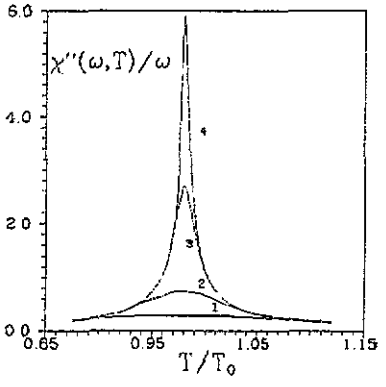

Figure 9. An illustration of a tendency to reach the master function for the imaginary part of susceptibility with a decrease of frequency. Here ω = 0.10(1); 0.001(2); 0.001(3); 0.0001(4).

transition. However, unlike that transition the freezing temperature τ_c^* does not depend on the measuring frequency. The important point to be decided is whether the experimentally found anomalies (the cusp behaviour) are connected with the dynamical freezing transition or with the thermodynamic glass transition.

Several attempts were made to describe the transitions in spin-glasses [33], in orientational glasses [34] and in polymers [35] in the framework of mode-coupling theory. This possibility has to be ruled out in the light of our results for the A-type freezing

transition. This means that all peaks in loss functions or the cusp-like points in real parts of the susceptibility suffering a clear frequency shift (e.g. by an Arrhenius or Vogel–Fulcher law) cannot be ascribed to a dynamical freezing transition found by the mode-coupling theory. These anomalies are caused by some other type of freezing kinetics, e.g. relaxation in a random potential landscape [7, 36].

We wish to emphasize again that, as far as it concerns the application of our results obtained in the framework of the mode-coupling approach, we look for a new kind of the freezing transition, which should take place above T_c in systems with usual structural phase transitions. For systems with a structural glass transition this dynamical transition should be searched for above the frequency-dependent thermodynamical glass transition point T_g. It is possible that this transition is not observable because of too strong an influence of the relaxing defects or hopping processes connected with correlated clusters. These effects are neglected in mode-coupling theory [10, 37, 38]. In principle there are two ways of overcoming these shortcomings of the theory.

First, following the phenomenological approach of [17] the relaxing defects can be included via the ansatz (cf (6))

$$M_{lk}(z) = \frac{\Delta_l}{\mathrm{i}z\tau_l + 1} + M^0_{lk}(z) \tag{35}$$

where $M^0_{lk}(z)$ is determined by (8). In the general case the parameter Δ_l and the relaxation time (e.g. $\tau_l = \tau_l^0 \exp(-E_a/k_B T)$) of a local relaxing defect are the random quantities. This additional relaxation process also yields an α-like loss peak at $T < T_c^*$ and can modify $\chi'(\omega, T)$ and $\chi''(\omega, T)$. For instance, the loss peak at T_c^* can be remarkably asymmetric [17].

Second, according to the generalized kinetic equation approach of [38, 39] hopping processes can be incorporated into by an improved expression for the relaxation kernel (7)

$$M_q(z) = M^0_q(z)/(1 - \delta_q(z) M^0_q(z)) \tag{36}$$

where the new kernel $\delta_q(z)$ contains the correlation functions of the type $(\dot{u}_l(t)|\dot{u}_k(0))$ $(\delta_q(z \to 0) \sim z)$. In consequence of this relaxation process the ideal central peak is smeared, i.e. at $T < T_c^*$ the α-like relaxation peak remains in $\chi''(\omega, T)$. This peak, however, does not show any critical scaling behaviour, as happens for systems with a broad distribution of relaxation times.

Hence under certain, not yet very clear, circumstances the typical scaling dynamics of the freezing transition can be masked and the critical scaling behaviour of α relaxation be not observable at all. In spite of that, the critical β relaxation should be seen in systems where the time constants of the hopping processes are large enough in comparison with the characteristic timescale $1/\omega_\beta$ of β relaxation. Therefore, the chance of finding a dynamical freezing transition increases if the measuring frequency is taken to be sufficiently high, but not too high.

So far, a clear indication that the freezing transition would take place has been observed only for supercooled liquids and polymers above T_g [10,16]. On the other hand, interesting data were obtained for a plastic crystal of difluortetrachlorethane (DFTCE). Using the Brillouin scattering technique ($\omega \sim$ 1–10 GHz) Krüger and co-workers [40, 41] detected a frequency-independent maximum in the damping $\Gamma(\omega, T)$ of longitudinal acoustic phonons and a first hint of the scaling behaviour $\Gamma(\omega, T) \sim (T - T_c^*)^{-\nu}$ for $T < T_c^* \approx$ 160–170 K. Furthermore, the longitudinal sound velocity changed its slope at T_c^*. Assuming a linear coupling of the order parameter and elastic degrees of freedom in this plastic crystal, a

change in eigenfrequencies ($\omega^2_{q,L} = C_L q^2$) and damping, $\Gamma(\omega, T)$, of longitudinal acoustic phonons can be determined via dynamical susceptibility as follows:

$$\Delta C_L(T) \sim \chi'(\omega_{q,L}, T) \qquad \Delta\Gamma(\omega, T) \sim \chi''(\omega, T)/\omega. \tag{37}$$

On the basis of these relations the Brillouin scattering results for DFTCE can be interpreted in the framework of the A-type freezing transition discussed above. In this connection it is worth noting that DFTCE possesses a real glass transition at $T_g = 90\,\mathrm{K}$, where the sound velocity experiences a cusp-like change and the specific heat nearly has a jump.

However, it is too early to make any final conclusions about this system. The experimental data must be carefully verified and a detailed analysis in terms of mode-coupling theory has to be made. This is work for the future.

We end this section with a remark on the attempts made to explain the central peak phenomenon by defect induced condensation. In [42] a theory was elaborated for unstable lattices with a finite concentration n of defects. This theory predicts a defect-induced phase transition at $T_c(n) > T_c(\text{pure})$, where the order parameter becomes substantially non-zero only at defect sites, but at $T \leqslant T_c(\text{pure})$ the whole system becomes long-range ordered. Interesting T, q and ω dependencies of the central component of the order parameter fluctuation spectrum were found. A striking difference from our theory is connected with the anomalous critical behaviour of the static susceptibility at $T_c(n)$. The mode-coupling theory for the dynamical freezing transition does not predict any anomalies in isothermal static susceptibility and only a cusp is allowed for the static limit of the dynamical response function. Therefore, a simple criterion can be used to distinguish between the dynamical freezing mechanism of mode-coupling theory and defect-induced condensation, proposed by Schwabl and Täuber [42]. To our knowledge the data on the static susceptibility for systems with a structural phase transition contain no indication of any remarkable anomalies above T_c. Therefore, we hope that the dynamical freezing transition is also to be observed in these systems.

5. Conclusions

The results of the numerical investigations of the ω and T dependence of the dynamical response function near T_c^* within the scalar φ^4-lattice model offers some suitable possibility for the experimental confirmation of the existence of the freezing transition above the temperature of the structural phase transition. The mode-coupling approach predicts either (i) a B-type transition in pure systems, where an α relaxation peak freezes in at T_c^*, or (ii) an A-type transition for the systems with strong enough defects, where the central peak begins to appear with zero intensity. It seems that the possibility of experimental observation appears more realistic in the latter case.

To the best of our knowledge the experimental data on the intensity of the central peak do not contain any direct information about the transition region $T \sim T_c^*$ [2, 3, 43]. A crude estimate of the central peak intensity always points to the A-type transition, if any freezing transition exists at all. The examples are the compounds $SrTiO_3$ [2, 3, 44], $RbCaF_4$ [3, 45], and the TSCC [43, 46, 47] samples.

In the case of a B-type freezing transition the temperature T_c^* lies very near the phase transition point T_c. Therefore, the critical fluctuations certainly mask the anomalous fluctuations that belong to the freezing transition. Nevertheless, a careful study of the ω-dependence of the order parameter susceptibility at temperatures $T > T_c$ might provide

some hint of the freezing transition occurrence. In particular, the existence of the scaling behaviour of two types around the α and β relaxations would give a strong indication of the new phenomenon taking place, though the mode-coupling theory may be too crude to correctly describe the scaling exponents [26].

In the case of an A-type transition the situation is more favourable for carrying out an experimental test. Here, the temperature T_c^* lies far from T_c so the critical fluctuations can be excluded. The T-dependence of the dynamical response function for the reasonably high measuring frequency ω must then reveal some peculiarities characteristic of the A-type freezing transition as such a transition occurs. The key point is the ω-independent position of the loss peak (or susceptibility cusp) at a sought-for temperature T_c^*, as well as the characteristic behaviour of the loss-peak wing.

As well as direct measurements of the order parameter susceptibility (mechanic, dielectric or magnetic) indirect measurements appear also very useful for the solution of the considered problem. First, we consider neutron and Brillouin scattering investigations [12, 13, 16, 48]. Other methods, like ultrasonic and NMR measurements, also offer ways of detecting anomalies of the above-considered kind at the freezing transition. A very good candidate to be used in the investigation of a freezing transition at $T_c^* > T_c$ is the TSCC compound [43, 46, 47]). TSCC is a strongly anisotropic system with a one-component order parameter, i.e. this system can be well described by the scalar φ^4-lattice model of structural phase transitions. In fact, in TSCC the central peak was found above T_c in the temperature range $T_c < T < T_c^* = T_c + \Delta T^*$, where $\Delta T^* \simeq 20\,\mathrm{K}$. An investigation of the ω and T dependence of the dynamical scattering function for this system, as was done for $Ca_{0.4}K_{0.6}(NO_3)_{1.4}$ by Cummins and co-workers [16], would be very interesting. A corresponding consideration of other systems with structural instability, especially of perovskites, would be also very desirable. In this connection it cannot be excluded that the recently found anomalies in dielectric [49], EPR [50], neutron scattering [51] and elastic [52] measurements on $SrTiO_3$ at $T_0 \simeq 40\,\mathrm{K}$ will be related to the dynamical freezing transition of the kind discussed above. Of course, in this case the quantum corrections have to be incorporated into some adequate theory [53]. As a result one may hope to find the answer to the still open question of the existence of the freezing transition in crystalline systems with structural phase transitions.

At that one should keep in mind the following circumstances. The dynamical scattering function is determined by the density–density correlation functions and can be approximated by the order parameter correlation function only in the lowest order. Therefore, it is necessary to include in the mode-coupling theory the higher-order fluctuation contributions. In principle it is possible that the freezing transition can be observed only due to these contributions [10]. We now deal with some theoretical approaches to this question.

As mentioned in section 4 it would be also of interest to reanalyse the experimental data obtained for crystalline or disordered systems showing a glass-like transition at the temperature T_g. An intriguing question is whether a dynamical freezing transition also occurs above the thermodynamic glass transition in such systems. The findings for DFTCE [40] are therefore of great importance and hence a detailed analysis of all available experimental data for DFTCE is very desirable. It would be important as well to clarify the differences and similarities between the freezing-like transition in DFTCE and in systems with an orientational glass transition [17] and a spin-glass transition. It is likely that in the latter case the kinetics in a fixed stochastic energy-barrier landscape dominate in the behaviour of the dynamical response function, and it might even happen that no dynamical freezing transition in the above sense takes place.

Finally, we want to point to the problem of clearing up the microscopic structure of the

frozen state at temperatures $T_{c(g)} < T < T^*_{c(g)}$. In the above-reported numerical treatment only the diagonal part of the relaxation function was taken into account. Exploiting the q-dependent diffuse scattering in the neutron or x-ray diffraction experiments one can obtain essential information on the correlated cluster formation in the quoted temperature range.

Acknowledgments

Stimulating discussions with Dr J Baschnagel, Professor W Götze, Professor R Schilling and Professor N M Plakida are gratefully acknowledged. We thank Dr S Flach for numerous useful comments. We feel indebted to Dr J-K Krüger for valuable comments on the experimental aspects of the theory. Our thanks are also due to Mrs T Drozdova for her help in the preparation of the English version of this paper. One of us (EIK) thanks the 'Deutsche Akademischer Austauschdienst (DAAD)' for financial support. The present work was partly supported by the VDI-Technologiezentrum Düsseldorf under project 01170/011.

References

[1] Müller K A 1979 *Dynamical Critical Phenomena and Related Topics* ed. C P Enz (Berlin: Springer) p 210
[2] Müller K A 1983 *Statics and Dynamics of Nonlinear Systems* ed G Benedek *et al* (Berlin: Springer) p 68
[3] Bruce A D and Cowley R A 1981 *Structural Phase Transitions* (London: Taylor and Francis)
[4] Aksenov V L, Bobeth M, Plakida N M and Schreiber J 1987 *J. Phys. C: Solid State Phys.* **20** 375
[5] Aksenov V L, Bobeth M, Plakida N M and Schreiber J 1987 *Z. Phys.* B **69** 393
[6] Bengtzelius U, Götze W and Sjölander A 1984 *J. Phys. C: Solid State Phys.* **17** 5915
[7] Palmer R G 1982 *Adv. Phys.* **31** 669
[8] Sidebottom D L and Sorensen C M 1993 (to be published)
[9] Angell C A 1988 *J. Phys. Chem. Solids* **49** 863
[10] Götze W 1991 *Liquids, Freezing and the Glass Transition* ed. J-P Hansen, D Levesque and J Zinn-Justin (Amsterdam: North-Holland) p 289
[11] Götze W and Sjögren 1989 *J. Phys.:Condens. Matter* **1** 4183
[12] Mezei F, Knaak W and Farago B 1987 *Phys. Scri.* T **19** 363
[13] Richter D (ed) 1989 *Dynamics of Disordered Materials* (Berlin: Springer)
[14] Richter D *et al* 1990 *Phys. Rev. Lett.* **64** 2921
[15] Petry W 1991 *Z. Phys.* B **83** 175
[16] Li G, Du W M, Chen X K and Cummins H Z 1992 *Phys. Rev.* A **45** 3867
[17] Bostoen C and Michel K H 1991 *Phys. Rev.* B **43** 4415
[18] Petry W *et al* 1991 *Phys. Rev.* B **44** 210
[19] Krumhansl J and Schrieffer J R 1975 *Phys. Rev.* B **11** 3535
[20] Mori H 1965 *Prog. Theor. Phys.* **33** 423; **34** 399
[21] Tserkovnikov Yu A 1981 *Theor. Math. Phys.* **49** 219
[22] Götze W 1985 *Z. Phys.* B **60** 195
[23] Flach S 1991 *Z. Phys.* B **82** 419
[24] Kob W and Schilling R 1991 *J. Phys.: Condens. Matter* **3** 9195
[25] Flach S, Siewert J, Siems R and Schreiber J 1991 *J. Phys.: Condens. Matter* **3** 7061
[26] Flach S and Siewert J 1992 *J Phys.: Condens. Matter* **4** L363
[27] Sen S, Cai Z X and Mahanti S D 1993 *Phys. Rev.* E **47** 273
[28] Fuchs M, Götze W, Hofacker I and Latz A 1991 *J Phys.: Condens. Matter* **3** 5047
[29] Press W H, Flannery B P, Teukolsky S A and Vetterling W T 1985 *Numerical Recipes: The Art of Scientific Computing* (Cambridge: Cambridge University Press)
[30] McCracken D D and Dorn W S 1965 *Numerical Methods and FORTRAN Programming* (New York: Wiley)
[31] Abramowitz M and Stegun I A 1984 *Pocketbook of Mathematical Functions* (Frankfurt: Deutsch)
[32] Götze W 1984 *Z. Phys.* B **56** 139
[33] Götze W and Sjögren L 1984 *J. Phys. C: Solid State Phys.* **17** 5759
[34] Michel K H 1987 *Z. Phys.* B **68** 259

[35] Sjögren L 1991 *J. Phys.: Condens. Matter* **3** 5023
[36] Binder K and Young A P 1986 *Rev. Mod. Phys.* **58** 811
[37] Götze W and Sjögren L 1988 *J. Phys. C: Solid State Phys.* **21** 3407
[38] Sjögren L 1990 *Z. Phys.* B **79** 5
[39] Sjögren L and Sjölander A 1979 *J. Phys. C: Solid State Phys.* **12** 4369
[40] Schreiber J, Krüger J-K, Jiminez R and Legrand J F 1991 *Proc. 2nd Meeting on Disorder in Molecular Solids, Garchy*
[41] Krüger J-K 1991 private communication
[42] Schwabl F and Täuber U C 1991 *Phys. Rev.* B **44** 11112
[43] Petzelt J *et al* 1990 *Solid State Commun.* **73** 5
[44] Currat R, Müller K A, Berlinger W and Denoyer F 1980 *Phys. Rev.* B **17** 2937
[45] Almairac A, Rousseau M, Gesland J Y, Nouet J and Hennion B 1977 *J. Physique* **38** 1429
[46] Pawlaczyk Cz and Unruh H G 1986 *Phys. Stat. Sol. (b)* **136** 435
[47] Petzelt J *et al* 1988 *Ferroelectrics* **80** 829
[48] Krüger J -K 1989 *Optical Techniques to Characterize Polymer Systems* ed. H Bässler (Amsterdam: Elsevier)
[49] Maglione M, Rod S and Hochli U T 1987 *Europhys. Lett.* **4** 631
[50] Müller K A, Berlinguer W and Tosatti E 1991 *Z. Phys.* B **84** 277
[51] Vacher R, Pelous J, Hennion B, Coddens G, Courtens E and Müller K A 1992 *Europhys. Lett.* **17** 45
[52] Nes O-M, Müller K A, Suzuki T and Fossheim K 1992 *Europhys. Lett.* **19** 397
[53] Flach S and Schreiber J 1987 *Phys. Stat. Sol. (b)* **140** K1